

Inside...

Visiting Fellows' Reports	2
Current Abstracts	3
New Visiting Fellows	8

The IRM Quarterly

Winter 1998-99, Vol. 8, No. 4 Institute for Rock Magnetism

Photograph by Christoph Geiss. Screenplay by Christoph Geiss, based on an original concept by Christoph Geiss. Produced and directed by Christoph Geiss.



Visiting Fellow **Ken Kodama** measuring magnetic properties of lacustrine sediments at very low temperature, using state-of-the-art instrumentation at IRM.

New Low-Temperature Measurement Capabilities

Mike Jackson
Jim Marvin
IRM

One step backward and two steps forward have resulted in a dramatic net increase in IRM's capabilities for magnetic measurements at very low temperatures.

Sensitive low-temperature measurements have become increasingly important in rock magnetism with the growing emphasis on sediments, as carriers of both environmental and paleomagnetic field information. Sediments are especially vulnerable to chemical/mineralogical alteration during high-temperature measurements, but by measuring at low temperatures we are able to extract critical information about magnetic mineralogy and particle size distributions *without* the risk of alteration.

Let's first dispose of the step backwards.

It was a dark and stormy night.

Our LakeShore AC susceptometer (see *Quarterly* v 4, n 1), unaware of any menace, was in the midst of a temperature sweep when the lights suddenly went out. Thunder rumbled in the distance. There was a moment of tense silence, which was punctured by a piercing scream.

Actually, it was just a routine power outage. Unfortunately, when the power was restored, the LakeShore temperature control system was unable to regain command of its sample-space heater, which melted a straw-and-gelcap sample assembly, and ruptured the seal that formerly isolated the sample space from the surrounding vacuum (thermal insulation) space.

Various attempts to repair the seal were temporarily successful. More

recently we have experimented with leaving the sample and vacuum spaces joined, sharing a helium gas pressure that is both sufficiently low to prevent excessive influx of ambient heat and sufficiently high to enable the sample to be raised from 20 K to room temperature. These experiments have produced encouraging results. However, if you are planning a visit and contemplating low-temperature susceptibility measurements, either (a) contact us for the latest developments, or (b) plan on using the Quantum Design instrument instead of the LakeShore.

Now for the good news.

It was a cold, bright sunny day when a truck full of large packing crates arrived, containing the newest instrument in the IRM orchestra: a Quantum Designs MPMS-XL (magnetic property measurement system, extra large). Mike Jones of Quantum arrived shortly thereafter for installation, initial testing and tuning, and in short order he had the system humming, with perfect pitch.

To be precise, it has a top frequency (for AC susceptibility measurements) of 1500 Hz, or approximately F#, and it extends down to a subaudible 10 mHz (E), giving a total range of more than twenty octaves. In this and all other characteristics, it mirrors our original MPMS (model 5S), with the exception of luminosity: its cabinet is equipped with a blinding red stripe, presumably to promote alertness.

AC applied-field amplitudes up to 240 A/m (3 Oe) are available on both Quantum instruments. For comparison, the LakeShore provides AC fields up to 1000 A/m, with frequencies from 10 Hz to 10 kHz (a bit more than an octave beyond the extremes of a piano, in both directions). LakeShore measurements are made in the frequency domain through a lock-in amplifier; in-phase ($\theta=0$) and quadrature ($\theta=90^\circ$) measurements are made separately, and any measurements of harmonics require a separate experiment. The Quantum instruments measure magnetization waveforms, from which in-phase, quadrature, and harmonic components may be calculated. Preliminary tests indicate that the noise floor is lower for the Quantum instruments, by at least a factor of two.

Both Quantum instruments of course also measure DC magnetic moments, and

Low-T

continued on page 7...

Visiting Fellows' Reports

Recent IRM research visits by **Özden Özdemir, David Dunlop, and Patrick Colgan** spanned much of the gamut of

rock magnetism: fundamental properties of magnetite crystals; experimental tests of TRM theory and the paleointensity

methods based thereon; and application of mineral magnetism and paleomagnetism to correlation and dating of tills.

David Dunlop

University of Toronto
dunlop@physics.utoronto.ca

Experiments on TRM and partial TRM in 125-150 μm magnetite grains

The main purpose of these experiments was to test the validity of Thellier's laws of additivity and independence of partial TRM's. Deviations from these laws compromise the determination of paleofield intensity by the Thellier method and the resolution of primary and secondary NRM's by stepwise thermal demagnetization.

The first test was the dependence of partial TRM intensities on initial state: AF demagnetized; TH - thermally demagnetized by cycling to T_c and back to T_o , then heated to T; TC - heated to T_c , then cooled to T. There is a consistent pattern (Table 1), as discovered earlier by Russian workers (e.g., Vinogradov & Markov, Invest. Rock Magn. Paleomagn., Inst. Phys. Earth, Moscow, 31-9 1989).

The differences reveal different starting local energy minimum (LEM) states. These may involve different numbers or configurations of domains, or different locations and pinning strengths of domain walls.

The second experiment was the dependence of total TRM on applied field strength from 0 to 1 mT. The field dependence of TRM potentially yields much information about domain state (SD, PSD, MD) (e.g., Dunlop & Argyle, J. Geophys. Res. 102, 20199-210, 1997). For the present magnetite grains, the TRM was most non-linear in small fields of <0.2 mT, comparable to the earth's field. TRM had a more linear field dependence in fields of 0.5-1 mT. This non-linearity in weak fields poses a problem for paleointensity determination, but is normal behavior for multidomain grains.

The third experiment was additivity of partial TRM's with the TC initial state (Table 2). The additivity is quite good, particularly for the lower T_i pairs of pTRM's.

In the final and main body of experiments, all the partial TRM's in the table were stepwise thermally demagnetized. The results answered two questions:

Table 1. pTRM intensities [emu] for different temperature ranges and initial conditions

pTRM (T, T_o , H)	AF state	TH state	TC state
300°C, 1 mT	4.09 E-4	4.39 E-4	5.31 E-4
400°C, 0.3 mT	1.75 E-4	1.73 E-4	1.95 E-4
500°C, 0.3 mT	1.95 E-4	2.14 E-4	2.69 E-4
564°C, 0.3 mT	3.63 E-4	3.76 E-4	4.22 E-4

Table 2. pTRM additivity.

T_i (°C)	pTRM (T_i, T_o)	pTRM (T_c, T_i)	Sum	Total TRM
300	5.31 E-4	18.66 E-4	23.97 E-4	24.44 E-4
400	1.95 E-4	6.74 E-4	8.69 E-4	8.71 E-4
500	2.69 E-4	6.25 E-4	8.94 E-4	8.71 E-4
564	4.22 E-4	5.01 E-4	9.23 E-4	8.71 E-4

(1) Does pTRM additivity hold throughout the unblocking process?

(2) Are adjacent pTRM's independent or do their Tub's overlap?

The answer to the first question is yes: the sum of the thermal demagnetization curves of pairs of adjacent pTRM's almost exactly matches the total TRM demagnetization curve, over the whole range from T_o to just below T_c .

This result is remarkable because the adjacent pTRM's are definitely not independent. At the boundary temperature T_i separating their T_b ranges, 20-23% of the lower pTRM remains undemagnetized, while 8-15% of the higher pTRM has already demagnetized below T_i , its minimum T_b . Thus there is substantial overlap of Tub's of the two partial TRM's. The overlap is not confined to a small range around T_i ; it extends practically all the way from T_o to T_c . Therefore there is no temperature range where an overprinted primary TRM could be cleanly isolated from the secondary thermal overprint by stepwise thermal demagnetization.

This is a serious practical problem for paleomagnetists. Probably only a supplementary cleaning method, such as prior low-temperature demagnetization (LTD) or partial AF cleaning, will yield cleanly separated primary and secondary NRM's if the carriers are multidomain grains. The LTD pre-treatment was tested in an earlier visit and shown to be effective. Complete AF demagnetization curves of all the pTRM's were

measured during the present stay. Unfortunately the higher pTRM's (T_c, T_i) are almost as easily AF demagnetized as the lower pTRM's (T_i, T_o). A good deal of supplementary knowledge about the particular pair of pTRM's would be needed in order to design an effective AF pre-treatment field.

A final aspect of pTRM additivity is the equivalence of vector and scalar sums of pTRM's. Secondary NRM's in nature are not usually parallel to the primary TRM they overprint. There may be a large angle between them (180° if the field has reversed). For $T_i = 400^\circ\text{C}$, I thermally demagnetized three different combinations:

(1) pTRM (T_c, T_i) + pTRM (T_i, T_o) in a single cooling, with the field rotated 90° at T_i ;

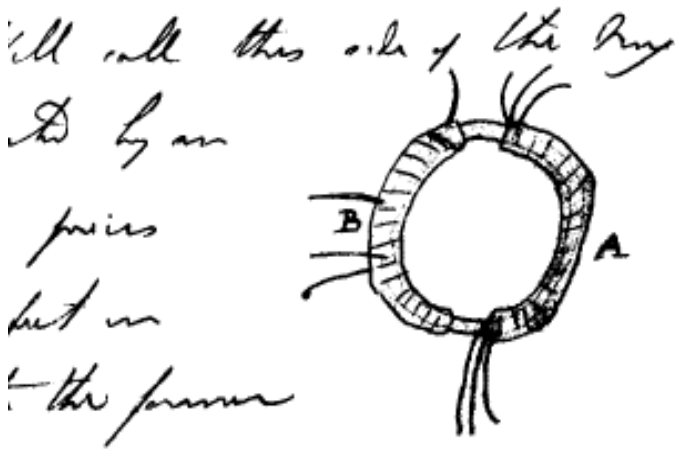
(2) TRM (T_c, T_o) + heating to T_i + pTRM (T_i, T_o), with the field rotated 90° at T_o after TRM production;

(3) a synthesized thermal demagnetization curve: an orthogonal combination of data for pTRM (T_c, T_i) and pTRM (T_i, T_o) produced in two separate runs.

The results were essentially indistinguishable within the experimental uncertainties. Other T_i 's and other angles need to be tested in further experiments.

Reports

continued on p. 6



"Aug 29th, 1831. Expts. on the production of Electricity from Magnetism, etc. Have had an iron ring made (soft iron)...6 inches in external diameter. Wound many coils of copper wire round one half... call this side of the ring A. On the other side but separated by an interval was wound wire... the direction being as with the former coils; this side call B... connected its extremities by a copper wire passing to a distance and just over a magnetic needle. Then connected the ends... on side A with battery; immediately a sensible effect... the helix strongly attracted the needle; after a few vibrations it came to rest in its original and natural position; and then on breaking the battery connection the needle was strongly repelled, and after a few oscillations came to rest in the same place as before." This was the first experimental demonstration of magnetic induction, i.e., generation of an electric current by a time-varying magnetic flux through a coil. [Faraday's Diary, Being the Various Philosophical Notes of Experimental Investigation Made by Michael Faraday During the Years 1820-1862, published by G. Bell & Sons, London, 1932.]

Current Abstracts

Environmental Magnetism

A list of current research articles on the physics and chemistry of natural magnetic materials is a regular feature of the IRM Quarterly. Articles published in familiar geology and geophysics journals are included; special emphasis is given to current articles from physics, chemistry, and materials-science journals. Most abstracts are culled from INSPEC (© Institution of Electrical Engineers), Geophysical Abstracts in Press (© American Geophysical Union), and The Earth and Planetary Express (© Elsevier Science Publishers, B.V.), after which they are condensed for this newsletter. Your contributions are always welcome.

Arnold, E., Merrill, J., Leinen, M., and King, J., 1998, **The effect of source area and atmospheric transport on mineral aerosol collected over the North Pacific Ocean:** *Global and Planetary Change*, v. 18, no. 3-4, p. 137-59.

Aerosol samples collected on two North Pacific cruises were analyzed for rock-magnetic properties, grain size and mineralogy. Aerosols originating from west of the Pacific are characterized by high coercivity, and are relatively enriched in kaolinite. Those originating from continents to the north and east of the Pacific basin contain coarse-grained material, have low coercivity, and are relatively enriched in plagioclase. Concentration of the mineral aerosol decreases with increasing transport time, and it is compositionally fractionated during transport, with a relative decrease in the primary minerals quartz and plagioclase and an increase in the smectite, illite and chlorite.

Kissel, C., Laj, C., Mazaud, A., and Dokken, T., 1998, **Magnetic anisotropy and environmental changes in two sedimentary cores from the Norwegian Sea and the North Atlantic:** *Earth and Planetary Science Letters*, v. 164, no. 3-4, p. 617-26.

Magnetic fabrics are oblate and the variations of the degree of anisotropy are climatically controlled, with higher values during short warm events or interglacial periods. It appears that, although a differential compaction might have been active, the fabrics mainly result from

depositional effects. The exact mechanisms of the link between magnetic fabrics and bottom current dynamics are, as yet, open to discussion.

Lean, C. M. B., and McCave, I. N., 1998, **Glacial to interglacial mineral magnetic and palaeoceanographic changes at Chatham Rise, SW Pacific Ocean:** *Earth and Planetary Science Letters*, v. 163, no. 1-4, p. 247-60. Mineral magnetic property measurements (ARM, SIRM, S ratio) show well-defined glacial-interglacial variability, interpreted as an interglacial increase of single domain magnetite grains. Examination by TEM of magnetic extracts reveals abundant cubic to octahedral grains of 0.02-0.2 μm size, often arranged in long chains characteristic of bacterial magnetite. It is suggested that during interglacials, with lower productivity (and organic carbon input to the bed), the oxic zone in the sediments is thicker and therefore is colonised longer by magnetite producers. This yields a climate-controlled stratigraphy which leads that of infaunal benthic foraminifera by no more than a few centimetres.

Rousseau, D. D., Zoller, L., and Valet, J. P., 1998, **Late Pleistocene climatic variations at Achenheim, France, based on a magnetic susceptibility and TL chronology of loess:** *Quaternary Research*, v. 49, no. 3, p. 255-63. A high-resolution analysis of magnetic susceptibility discloses a fine-grained "marker" horizon, interpreted as a small-scale dust layer deposited prior to the main interval of loess deposition. New thermoluminescence dates indicate that the loess deposition took place after the MIS 5/4 boundary, i.e., after 70 kyr. On a more regional scale, the Achenheim loess sequence demonstrates a reliable correlation between the western side of the Eurasian loess belt and the dust record of the Greenland ice cores.

Xiao-Min, F., Ji-Jun, L., and Van der Voo, R., 1999, **Rock magnetic and grain size evidence for intensified Asian atmospheric circulation since 800,000 years B.P. related to Tibetan uplift:** *Earth and Planetary Science Letters*, v. 165, no. 1, p. 129-44.

Paleomagnetic, rock magnetic, and grain size studies of a thick loess sequence in the West Qin Ling (mountain range) suggest (1) that Asian air circulation may have changed and intensified at about 800 ka resulting in dust deposition in West Qin Ling; (2) that dust-carrying winds were driven not only by the Asian winter monsoon, but included also the westerlies and a winter monsoon caused by the Tibetan Plateau High, and (3) that intensification of all these air circulation systems continues to the present.

Extraterrestrial Magnetism

Bradley, J. P., McSween, H. Y., Jr., and Harvey, R. P., 1998, **Epitaxial growth of nanophase magnetite in Martian meteorite Allan Hills 84001: implications for biogenic mineralization:** *Meteoritics & Planetary Science*, v. 33, no. 4, p. 765-73.

Analytical electron microscopy shows individual magnetite nanocrystals on the surfaces of carbonates epitaxially intergrown with one another in "stacks" of single-domain crystals. Other magnetite nanocrystals are epitaxially intergrown with the surfaces of the

carbonate substrates. Epitaxy rules out intracellular precipitation of these magnetites by (Martian) organisms, provides further evidence of the high-temperature (>120°C) inorganic origins of magnetite in ALH 84001, and indicates that the carbonates also have been exposed to elevated temperatures.

Crary, F. J., and Bagenal, F., 1998, **Remanent ferromagnetism and the interior structure of Ganymede:** *Journal of Geophysical Research*, v. 103, no. E11, p. 25757-73. An active dynamo is not necessary to produce Ganymede's magnetic fields. The rocky material within Ganymede is believed to be rich in iron-bearing minerals, particularly magnetite, and its outer layer is capable of holding strong remanent magnetism. Two possible sources of remanent ferromagnetism are an extinct internal dynamo, and Jupiter's (paleo)magnetic field. A model of remanent magnetization shows that magnetization by the jovian background field can account for no more than 5.6% of Ganymede's internal field. However, a paleomagnetic field comparable to the Earth's current field is capable of producing sufficient remanent magnetization to account for the Galileo observations.

Hong, Y., and Fegley, B., Jr., 1998, **Experimental studies of magnetite formation in the solar nebula:** *Meteoritics & Planetary Science*, v. 33, no. 5, p. 1101-12.

Fe metal and Gibeon meteorite metal were experimentally oxidized to magnetite, identified by X-ray diffraction. The experimental data are used to model the reaction time of Fe alloy grains in the solar nebula as a function of grain size and temperature. The reaction times for 0.1-1 μm metal grains are generally within estimated lifetimes of the solar nebula (0.1-10 Ma).

Morris, R. V., Golden, D. C., Shelfer, T. D., and Lauer, H. V., Jr., 1998, **Lepidocrocite to maghemite to hematite: a pathway to magnetic and hematitic Martian soil:** *Meteoritics & Planetary Science*, v. 33, no. 4, p. 743-51.

Lepidocrocite was heated in air at temperatures up to 525°C, and the decomposition products analyzed by XRD, TEM, magnetic methods, and reflectance spectroscopy. Single-crystal lepidocrocite particles dehydroxylated to polycrystalline particles of disordered maghemite that subsequently transformed to polycrystalline particles of hematite. These experiments are consistent with lepidocrocite as the precursor of Mh+Hm assemblages on Mars, but other phases (e.g., magnetite) that decompose to Mh and Hm are also possible precursors.

Werner, T., and Borradaile, G. J., 1998, **Homogeneous magnetic susceptibilities of tektites: implications for extreme homogenization of source material:** *Physics of the Earth and Planetary Interiors*, v. 108, no. 3, p. 235-43.

Low field magnetic susceptibility of tektites from the Australasian strewn field is weak, dominated by paramagnetism of the silicate glass. Susceptibilities calculated from the large number of published geochemical analyses yield similar low values. To produce susceptibilities

Abstracts

continued on p. 4

in such a narrow range ($50\text{-}100 \times 10^{-9} \text{ m}^3 \text{ kg}^{-1}$) requires a target source that is both appropriate and widespread over the Earth's surface. Modern marine sediments would appear to fill these requirements.

Xin, H., and Buseck, P. R., 1998, **Unusual forms of magnetite in the Orgueil carbonaceous chondrite**: *Meteoritics & Planetary Science*, v. 33, no. 4, suppl.iss, p. A215-20. The Orgueil CI carbonaceous chondrite contains magnetite (Fe_3O_4) that displays a rich and seemingly unique variety of morphologies. Recent images show unambiguous trapezohedral crystals and possibly also trisectahedral forms. Although magnetite is an extremely abundant terrestrial mineral and commonly occurs in well-developed crystals, neither of these forms has been recognized previously. The barrel-shaped arrays of magnetite discs ("plaquettes") are also unique. Their morphologies and association with sulfates and carbonates suggest an aqueous origin.

Magnetic Microscopy and Spectroscopy

Fabris, J. D., Coey, J. M. D., and Mussel, W. d., 1998, **Magnetic soils from mafic lithodomains in Brazil**: *Hyperfine Interactions*, v. 113, no. 1-4, p. 249-58.

Tropical soils typically retain high amounts of iron oxides, some of them magnetic. The two major orders forming on mafic domains, namely, dusky red Oxisol and Alfisol, generically referred to as *terrae rossae*, are the most representative magnetic soils and cover as much as 3.9% of the Brazilian land area. In this paper, an up-to-date overview is presented, dealing with selected magnetic soils forming on four representative examples of mafic lithology.

Garvie, L. A. J., and Buseck, P. R., 1998, **Ratios of ferrous to ferric iron from nanometre-sized areas in minerals**: *Nature*, v. 396, no. 6712, p. 667-70.

Many mineral samples are too fine-grained and heterogeneous to be studied by standard methods such as Mössbauer spectroscopy, electron microprobe, and wet chemistry. Electron energy-loss spectroscopy can be used with a transmission electron microscope to determine $\text{Fe}^{3+}/\Sigma \text{Fe}$ minerals at the nanometre scale. This procedure is efficient for determining $\text{Fe}^{3+}/\Sigma \text{Fe}$ ratios of minor and major amounts of iron on a scale heretofore impossible and allows information to be obtained not only from ultra-fine grains but also, for example, at reaction fronts in minerals.

Medrano, C., Heyroth, F., Schlenker, M., Baruchel, J., and Espeso, J., 1998, **Two- and three-beam X-ray diffraction imaging of domains in magnetite**: *Journal of Applied Crystallography*, v. 8898, no. 98, p. 0021-8898.

The X-ray diffraction topographic imaging process for ferrimagnetic domains in magnetite Fe_3O_4 at room temperature is investigated, in two- and three-beam cases, for incident synchrotron radiation beams differing in angular divergence and energy spread. A three-beam Umweganregung case involving the weak 171 and the strong 131 reflections shows unusual domain contrast on the 171 topographs, even on images involving energy or angle

integration; this contrast is particularly evident on white-beam topographs. The high angular sensitivity this implies is associated with the difference in dispersion relation between the two reflections.

Medrano, C., Schlenker, M., Baruchel, J., Espeso, J., and Miyamoto, Y., 1999, **Domains in the low-temperature phase of magnetite from synchrotron-radiation X-ray topographs**: *Physical Review B*, v. 59, no. 2, p. 1185-95.

Domains in the low-temperature phase of magnetite Fe_3O_4 were investigated, via their ferroelastic distortion, by means of synchrotron radiation X-ray topography, complemented by Nomarski optical microscopy on the surface. After cooling through the Verwey transition under a magnetic field parallel to [001], the images show a hierarchy of domains. Domains associated with a small difference in lattice distortion provide a clear indication that the symmetry is triclinic. They appear as a substructure of monoclinic domains separated by walls creating no long-range stress. The domain structure deduced from the observation, under the experimentally self-tested assumption that the walls involved are stress free, is favorable from the elastic, magnetostatic, and electrostatic points of view.

Modeling and Theory

Kodama, R. H., and Berkowitz, A. E., 1999, **Atomic-scale magnetic modeling of oxide nanoparticles**: *Physical Review B*, v. 59, no. 9, p. 6321-36.

Spin distributions and net magnetic moments are calculated for nanoparticles of ferrimagnetic NiFe_2O_4 and $\gamma\text{-Fe}_2\text{O}_3$, and antiferromagnetic NiO as a function of applied field. Calculations incorporate crystal structures and exchange parameters determined from bulk data, bulk anisotropy for core spins, reasonable estimates for the anisotropy of surface spins, and finite temperatures simulated by random perturbations of spins. Simulated thermal perturbations were used to characterize the distribution of energy barriers between surface spin states of such particles. The distribution of barriers can explain the macroscopic quantum tunneling like magnetic relaxation at low temperatures found experimentally.

Newell, A. J., and Merrill, R. T., 1999, **Single-domain critical sizes for coercivity and remanence**: *Journal of Geophysical Research*, v. 104, no. B1, p. 617-28.

There are different SD size ranges for coercivity and for saturation remanence, with respective critical sizes $\text{LSD}_{\text{coerc}}$ and LSD_{rem} . To calculate the critical sizes, the authors use rigorous nucleation theory and obtain analytical expressions, allowing exploration of the effects of grain shape, stress, crystallographic orientation and titanium content in titanomagnetites. The size range for SD coercivity is always small, but the size range for SD remanence can vary enormously depending on the anisotropy. If the easy axes are oriented favorably, the SD state can occur in large $x=0.6$ titanomagnetite grains. Ensembles of magnetite grains with aspect ratios greater than 5 have SD-like remanence but low coercivity. However, most synthetic magnetite grains are nearly equant, and the predicted size range for SD remanence is small to nonexistent. This,

rather than grain interactions, may be the reason they have properties such as saturation remanence that do not agree well with standard SD theory.

Remanence and Magnetization Processes

Chong-Shern, H., Masayuki, T., Kai-Shuan, S., and Shuh-Ji, K., 1998, **Inconsistent magnetic polarities between greigite- and pyrrhotite/magnetite-bearing marine sediments from the Tsailiao-chi section, southwestern Taiwan**: *Earth and Planetary Science Letters*, v. 164, no. 3-4, p. 467-81.

Paleomagnetic samples from 65 sites in a 620-m-thick Middle to Late Pleistocene mudstone sequence revealed two types of thermal demagnetization ($25\text{-}400^\circ \text{C}$) behavior: (1) single-component stable remanence in magnetite- and pyrrhotite-dominated samples, and (2) two antiparallel remanence components in samples with significant greigite concentrations. The low-temperature ($< 340^\circ \text{C}$) component in the latter samples resides in greigite. This could have resulted either from delayed formation of greigite or from self-reversal during formation.

Hagstrum, J. T., and Sedlock, R. L., 1998, **Remagnetization of Cretaceous forearc strata on Santa Margarita and Magdalena islands, Baja California Sur: implications for northward transport along the California margin**: *Tectonics*, v. 17, no. 6, p. 872-82.

Paleomagnetic data indicate that these rocks have been remagnetized, probably during the Late Cenozoic. Widespread remagnetizations could have resulted from regional burial and uplift, related to changes in subduction parameters. Two episodes of remagnetization are apparent: one in the Late Cretaceous and a second in the Late Cenozoic. Unremagnetized and apparently reliable data from sedimentary and plutonic rocks on the Baja Peninsula consistently indicate northward translation ($14^\circ \pm 3^\circ$) and clockwise rotation ($29^\circ \pm 8^\circ$) with respect to North America since the Late Cretaceous.

Katz, B., Elmore, R. D., and Engel, M. H., 1998, **Authigenesis of magnetite in organic-rich sediment next to a dike: implications for thermoviscous and chemical remagnetizations**: *Earth and Planetary Science Letters*, v. 163, no. 1-4, p. 221-34.

Rock magnetic results from organic-rich sediment around a Tertiary dike in Scotland indicate changes in magnetic mineralogy and magnetite content as well as grain size in the contact zone. Chemical processes were an important contributor to the magnetization in the contact zone of the dike, but magnetite authigenesis was triggered by the heat of the intrusion rather than hydrothermal fluids. The results of this study suggest that moderately elevated burial temperatures might be sufficient to cause magneto-chemical changes, and that externally derived fluids may not be needed to cause authigenesis and remagnetization.

Menyeh, A., and O'Reilly, W., 1998, **Thermoremanence in monoclinic pyrrhotite particles containing few domains**: *Geophysical Research Letters*, v. 25, no. 18, p. 3461-4. The intensity of TRM acquired by synthetic

Fe₇S₈ particles in the size range 1-29 μm falls, and the unblocking temperature increases, with increasing particle size. The data can be fitted to a theory in which a fraction of the particles fails to nucleate a domain wall on cooling, only if the TRM of the resultant monodomain fraction is much smaller than that expected of crystals of this size. This could arise if the particles were made of "nanocrystals" of much smaller size. A simpler theoretical description adopts a particle-size-dependent effective demagnetizing factor with a fully formed domain structure with highly mobile walls above the blocking temperature.

Sagnotti, L., and Winkler, A., 1999, **Rock magnetism and palaeomagnetism of greigite-bearing mudstones in the Italian peninsula:** *Earth and Planetary Science Letters*, v. 165, no. 1, p. 67-80.

In agreement with previous studies of greigite, these sediments display: thermal decomposition of the magnetic carriers at temperatures above 230° C, resulting in decreased magnetic susceptibility values and maximum unblocking temperatures mostly in the range 320-350° C; high saturation isothermal remanent magnetization to low-field magnetic susceptibility ratios; hysteresis ratios that are typical for single domain (SD) grains; moderate coercivity, with coercivity of remanence between 52 and 81 mT; and a tendency to acquire a significant rotational remanent magnetization. Greigite-bearing sediments are particularly sensitive to field impressed anisotropy, enabling definition of a new magnetic parameter that can be used as a rapid means to screen a rock sample for the presence of greigite.

Tarduno, J. A., Wenlai, T., and Wilkison, S., 1998, **Biogeochemical remanent magnetization in pelagic sediments of the western equatorial Pacific Ocean:** *Geophysical Research Letters*, v. 25, no. 21, p. 3987-90. In sediments of ODP Site 805, biogenic magnetite found near the Fe-redox boundary carries a natural remanence. Because the production of biogenic magnetite is tied to the geochemical zonation of the sediments, we call this magnetization a biogeochemical remanence. These data indicate that some pelagic sediments can continue to acquire remanence significantly after the post-depositional lock-in of detrital magnetic grains.

Xiaodong, T., and Kodama, K. P., 1998, **Compaction-corrected inclinations from southern California Cretaceous marine sedimentary rocks indicate no paleolatitudinal offset for the Peninsular Ranges terrane:** *Journal of Geophysical Research*, v. 103, no. B11, p. 27169-92. The anisotropy of anhysteretic remanence was used to correct the inclinations of the Ladd and Point Loma formations from southern California. Individual magnetic grain anisotropy was determined by both compaction experiments and redeposition of a magnetic separate in a DC magnetic field. The mean inclination of the Ladd Formation was corrected from 46° to 58°, and that of the Point Loma from 39.5° to 56.0°. These results suggest that the Peninsular Ranges-Baja Borderland terrane has been part of the western North America since the Late Cretaceous and that clay-containing sedimentary rocks may typically experience from 10° to 15° of inclination shallowing due to burial compaction.

Synthesis and Properties of Magnetic Minerals

Adnan, J., and O'Reilly, W. O., 1999, **The transformation of γ-Fe₂O₃ to α-Fe₂O₃: thermal activation and the effect of elevated pressure:** *Physics of the Earth and Planetary Interiors*, v. 110, no. 1-2, p. 43-50.

The transformation of acicular γ-Fe₂O₃ particles to α-Fe₂O₃ is thermally activated. The energy barrier arises from the combination of a term representing the reduction in lattice energy in an inverted region, and the strain energy associated with the interface between the inverted and non-inverted phases. The sensitivity of the inversion process to pressure can be understood in terms of the dependence of these energy terms on interatomic spacing. Extrapolation of these laboratory data to the conditions of the submarine crust at Site 504B of the Deep Sea Drilling Project is consistent with the inferred magnetic mineralogy of the recovered material.

Hayashi, M., Susa, M., and Nagata, K., 1999, **Magnetic structure of as-quenched silicate glasses containing iron oxides:** *Journal of Applied Physics*, v. 85, no. 4, p. 2257-63.

The effect of valence states of iron on the magnetic structure of as-quenched silicate glasses containing iron oxides has been investigated. DC magnetizations and AC susceptibilities of the glasses are explained by a magnetic structure model in which both microcrystalline clusters and free iron ions in the glass matrix bear magnetism. The number density of microcrystalline clusters is highest in a sample of x=0.73 (x: the ratio of Fe³⁺ ions to the total number of iron ions). The average magnetic interaction among free iron ions in the glass matrix is stronger in the samples having larger values of x.

Lembke, U., Hoell, A., Kranold, R., Muller, R., Schuppel, W., Goerigk, G., Gilles, R., and Wiedenmann, A., 1999, **Formation of magnetic nanocrystals in a glass ceramic studied by small-angle scattering:** *Journal of Applied Physics*, v. 85, no. 4, p. 2279-86.

Nanosized crystallites of magnetite, Fe₃O₄, formed by heat treatment of a glass containing iron oxide, have magnetic properties that strongly depend on the heat treatment conditions. The size distribution of the nanocrystallites studied by small-angle X-ray scattering (SAXS) is bimodal. Small-angle neutron scattering (SANS) results reveal that both sizes are superparamagnetic. The volume distributions derived from magnetic SANS revealed peaks at smaller radii than those from nuclear SANS and SAXS data. Therefore, we suggest that a nonmagnetic surface layer surrounds the cores of the magnetite nanocrystals.

Mekki, A., and Ziq, K. A., 1998, **Magnetic properties of a SiO₂-Na₂O-Fe₂O₃ glass:** *Journal of Magnetism and Magnetic Materials*, v. 189, no. 2, p. 207-13.

A homogeneous SiO₂-Na₂O-Fe₂O₃ glass containing 4.6% Fe₂O₃ was prepared and devitrified to produce a glass ceramic containing the magnetic compound Na₅Fe(SiO₃)₄. DC magnetic susceptibility shows that the magnetic ion-ion interaction is antiferromagnetic. M(H) data at different temperatures do not collapse to a single curve in

the M(H/T) representation. The M(H) curves were fitted with Brillouin function by keeping the total number of magnetic ions constant and varying the proportion of ferrous ions until a best fit was achieved. The Fe²⁺/Fe_{total} ratio obtained from the fit is in good agreement with the value obtained from X-ray photoelectron spectroscopy (XPS).

Özdemir, Ö., and Dunlop, D. J., 1999, **Low-temperature properties of a single crystal of magnetite oriented along principal magnetic axes:** *Earth and Planetary Science Letters*, v. 165, no. 2, p. 229-39.

In an oriented 1.5-mm single crystal of magnetite, M(H) between 300 K and 10 K exhibits uniaxial symmetry below the Verwey transition temperature, T_v=119 K. The room-temperature SIRM produced along [001] decreases continuously during zero-field cooling to the isotropic temperature, T_i=130 K. At T_i, 86% of the initial SIRM was demagnetized. The domain wall pinning responsible for this soft remanence fraction must be magnetocrystalline controlled. The remaining 14% of the SIRM is temperature independent between T_i and T_v and must be magnetoelastically pinned. This surviving hard remanence is the core of the stable magnetic memory. The Verwey transition is marked by a discontinuous increase in remanence, indicating that the cubic [001] direction suddenly becomes an easy direction of magnetization.

Sorescu, M., Brand, R. A., Mihaila-Tarabasanu, D., and Diamandescu, L., 1998, **Synthesis and magnetic properties of haematite with different particle morphologies:** *Journal of Alloys and Compounds*, v. 280, no. 1-2, p. 273-8.

Haematite particles of four different morphologies (polyhedral, platelike, needlelike and disk-shaped) were synthesized by the hydrothermal method. The morphology and average particle diameter (1.4; 7.4; 0.2 and 0.12 μm, respectively) were determined by TEM combined with electron diffraction. The samples were studied by transmission Mössbauer spectroscopy in the temperature range 4.2-300 K. In all cases, a weak ferromagnetic phase (WF) was present above the Morin temperature of 230 K and found to coexist with an antiferromagnetic phase (AF) below this temperature. However, the populations of the two phases at 230 K were demonstrated to depend on the morphology of the particles.

Özden Özdemir

University of Toronto
 özdemir@
 physics.utoronto.ca

Low-Temperature Properties Of An Oriented Multidomain Magnetite

I measured saturation induced and remanent magnetizations and induced magnetization as a function of field at low temperatures, between 300 K and 10 K, using the MPMS. The experiments were carried out on a well characterized and an oriented 1.5 mm single crystal of magnetite.

Below the Verwey transition ($T_v=120$ K) magnetite is monoclinic, its a, b and c axes corresponding to the [1-10], [110] and [001] directions of cubic magnetite above T_v . The single crystal was oriented successively along these three principal axes for measurements. The c-axis is the direction of easiest magnetization below T_v ; a and b are hard and intermediate directions. The monoclinic c-axis may develop in any of the three equivalent $\langle 001 \rangle$ axes. A pre-determined c-axis was obtained by cooling through T_v in a field of 2.5 T applied along the [001] direction.

We have found that the induced magnetization curves at 10 K have quite different approaches to saturation. Saturation was achieved in relatively low fields of 0.2 T in the [001] easy direction but required much higher fields along the a and b axes. These results indicate that the crystal below T_v has essentially uniaxial symmetry.

We have also measured the temperature dependence of saturation magnetization along the three principal axes during cooling from 300 K to 10 K in a field of 2 T. The saturation magnetization increases with decreasing temperature in all three crystallographic orientations. The nearly identical curves show that cubic magnetite is magnetically isotropic above the Verwey transition.

Below T_v , the $M_s(T)$ curves are different for the a, b and c axes. In cooling through the Verwey transition, M_s dramatically decreases by 1.6% and 1.2% along a and b axes, respectively. The applied field during cooling was not enough to saturate the magnetization along these axes. Along the monoclinic c-axis, the field of 2 T is enough to saturate the magnetization of monoclinic magnetite. The $M_s(T)$ curve has only very small (~0.1%) discontinuity at the Verwey transition. The results also confirm that the magnetic symmetry is uniaxial below T_v .

The crystal was given an SIRM parallel to the monoclinic c-axis [001] in a field of 2.5 T at room temperature, then cooled to 10 K and warmed back to 300 K in zero field. The remanence decreased steadily with cooling to the isotropic temperature, $T_i=130$ K, where the first magnetocrystalline anisotropy constant K_1 becomes zero. At T_i , 86% of the original SIRM had been demagnetized. There was no further demagnetization between the isotropic point and the Verwey transition at $T_v=119$ K. The residual 14% of the original SIRM remained constant. These observations

indicate a sharp separation between the two remanence transitions, at T_i and T_v , which has not been clear in previously published data on unoriented crystals. In cooling to the isotropic point, the magnetocrystalline anisotropy decreases to zero and loosely pinned domain walls unpin, causing a large loss of remanence. Then at $T_v=119$ K, there is a crystallographic phase transition in which magnetite transforms from cubic spinel to monoclinic structure. An abrupt increase in the remanence in cooling through the Verwey transition clearly indicates that [001], the monoclinic c-axis, has suddenly become an easy direction of magnetization. In cooling through the Verwey transition, the SIRM increased from 0.005 to 0.081 Am²/kg. This is about 35% higher than the initial SIRM at 300 K.

As the crystal was warmed from 10 K, the remanence retraced the cooling curve. Thus the process affecting the remanence of the monoclinic magnetite below T_v is reversible. The remanence recovered by the cubic magnetite above T_v is identical to the remanence before cooling through T_v and remains constant during warming to 300K. All of the irreversible change in remanence occurred during zero field cooling to T_i . Thus the low temperature demagnetization (LTD) is governed entirely by the vanishing of magnetocrystalline anisotropy at T_i . The remaining 14% of the room temperature SIRM is due to strongly pinned domain walls, probably pinned magnetostrictively by dislocations or other crystal defects. This is the source of single domain-like memory observed in large single crystal of magnetite (Özdemir and Dunlop, 1998).

Patrick M. Colgan

Northeastern University
 pcolgan@lynx.dac.neu.edu

Rock magnetic properties and paleomagnetism of tills from Boston Harbor, Massachusetts

During my week-long visit to the IRM in September I was able to learn about and measure many rock magnetic parameters for glacial till samples from Boston Harbor, MA. The age of the older of the two tills is not known and preliminary data collected in the fall of 1997 showed some samples had a reversed polarity. I wanted to characterize the magnetic properties of each till and see if there were differences that might help with correlation between exposures as well as to determine the carrier of remanent magnetism. I also wanted to use rock magnetic properties to characterize a paleosol that is present between the two tills. Finally, I brought about 60 oriented samples to do step-

wise AF demagnetization and determine remanent magnetism of the lower till.

The equipment used by myself and my assistant Scott Lundin included the superconducting rock magnetometer (SRM), vibrating sample magnetometers (VSM and mVSM), kappa bridge, magnetic properties measurement system (MPMS), Lakeshore low-temperature AC susceptometer, and the AC anisotropy of magnetic susceptibility bridge (roly-poly) for measuring magnetic fabric. Learning how to use each piece of equipment was made painless by lots of help from IRM's staff. We worked fairly continuously for seven days and after a while felt like we were working in a factory as we made numerous measurements. I found working at the IRM kind of like spelunking, you have a tendency to lose track of time when isolated from day and night cycles for a long period of time.

The first goal of characterizing the

rock magnetic properties of the tills was very successful. Data from the Lakeshore showed little frequency dependence in any of our samples eliminating the possibility of single domain magnetite. The kappa-bridge and the MPMS showed that titanomagnetite was the main magnetic mineral present with some minor hematite. The magnetite is almost certainly detrital in origin and is probably the carrier of remanent magnetism (as detrital remanent magnetism DRM, or post-depositional remanent magnetism pDRM). The mVSM showed that pseudo-single domain magnetite was dominant in both tills.

Our second goal of trying to detect the paleosol was not achieved as there turned out to be little single domain magnetite in the paleosol samples. This is probably because the paleosol is truncated by the overlying till and only the C-horizon is present at the sampled

sections. The VSM and mVSM showed little difference between upper and lower tills. We do see differences in mass susceptibility and ARM in upper and lower tills. The paleosol did show some subtle differences in Hc and high-field slope. This may be a result of hematite or another high coercivity mineral being present in this zone as well as differences in clay mineralogy. Magnetic fabric was measured on the roly-poly and in many instances was very nearly the same as macro-fabric measured at the same sections.

Almost all (about 95%) of the samples run on the SRM showed a normal polarity, only a few samples showed a component of reverse polarity. These reverse samples may be the result of incorporation of preexisting blocks of

till (eroded, rotated, and deposited) as the reverse was seen in multiple samples within a single bed. It is also possible they are related to a reversal event, but so far we don't see a good stratigraphic pattern. Since new amino-acid age data on marine bivalve shells within the till suggest an early Pleistocene age for our samples, normal polarity is to be expected. We did see some shifts in declination in two sections, and we are hoping that we may be able to use the declination changes to correlate between individual units exposed in Boston Harbor.

I also carried out some experiments on the SRM to see what the effects of small pebbles were on the remanent magnetism. The most common pebble

in the till is an argillite (about 90% of all pebbles). These pebbles have a very weak remanent magnetization so probably add little to the DRM or pDRM recorded by pseudo-single domain magnetite. A few samples contain basalt and gabbro pebbles, but these are present in low percentages (< 2%). These pebbles have a very strong remanent magnetism and can contribute greatly to the measured paleomagnetism. Because of this I now screen my samples by determining their mass susceptibility. I have found that samples with basalt or gabbro pebbles have mass susceptibilities of about two to five times that of samples that do not.

My trip to IRM was very worthwhile in both new techniques learned and data collected. Thanks to all at the IRM who made our visit both productive and enjoyable.

...Low-T

continued from page 1

both feature the reciprocating-sample option (RSO) for greater sensitivity in measuring weak samples. In standard (non-RSO) DC measurements, the sample is moved upward in a series of steps through the SQUID pickup coils, the voltage is determined as a function of position, and the moment is determined by curve-fitting. RSO measurements achieve greater sensitivity by placing the sample at the position of maximum slope in the SQUID response curve (where sensitivity is maximum), oscillating it vertically, and measuring the SQUID output through a lock-in sensor (see figure). The RSO measurement head, unlike the standard head, has no sliding-seal airlock*, which has two

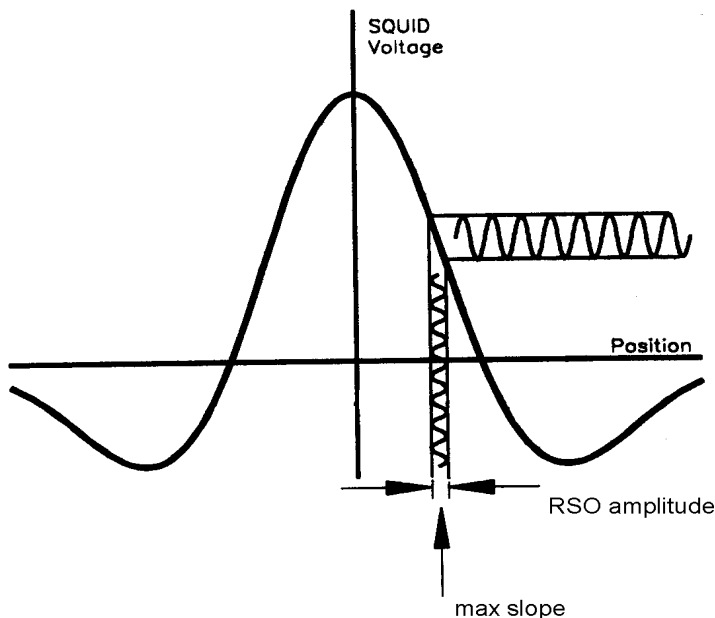
practical consequences: (+) leakage of air into the sample space is minimized, reducing problems due to freezing; and (-) the sample space must be brought to room temperature for sample removal/installation.

Probably the most important advantage of the new XL and the upgraded 5S is the improved temperature control. In particular, it is now possible to maintain temperatures below 4 K for extended periods, and to sweep smoothly through that critical temperature. More importantly, measurements can now be made while cooling. This is critical for distinguishing among a variety of mechanisms that can lead to remanence loss while warming in zero-field from low temperatures, including thermal unblocking, Curie/Néel transitions,

isotropic points and phase transitions. Only the latter two of these are "visible" in zero-field cooling experiments. Conversely, certain phenomena such as the Morin transition of hematite are more readily observed by cooling a room-temperature remanence (since hematite is a pure antiferromagnet below the transition, and thus carries no low-temperature remanence, so it is "invisible" in warming experiments).

A more subtle benefit of the new measure-while-cooling capability was discovered by one of the first users of the 5S after its upgrade. Özden Özdemir found that although warming curves for a single-crystal magnetite showed only a stark drop at the Verwey

SQUID RESPONSE



Low-T

continued on page 8...

Faraday, Michael

b. Sept. 22, 1791, Newington Butts; d. Aug. 25, 1867, Hampton Court

Faraday, with little formal education, developed an interest in the experimental study of nature while working as a bookbinder's apprentice. He was hired at the age of 21 by Sir Humphrey Davy as his laboratory assistant at the Royal Institution, and remained there for most of his life, making pioneering contributions to chemistry and electromagnetism. In 1831 he discovered electromagnetic induction and quantified it (Faraday's Law). He developed the concept of "lines of force," built the first dynamo, coined the term "diamagnetism" and investigated the phenomenon, and discovered the Faraday Effect (rotation of light polarization by a magnetic field). The SI unit of capacitance (1 farad = 1 coulomb/volt) is named for Faraday.

Spring/Summer Visiting Fellows

Next application
deadline: June, 1999.

The December deadline for Visiting Fellow applications yielded an extraordinary group of proposals, both in number and in overall quality. The IRM's Review and Advisory Committee had a difficult task in ranking them, and several members offered the opinion that this was the best overall group we have yet received. Unfortunately, we were not able to accept all of the worthwhile projects this time, but some new instrumentation (see cover story for details) has enabled us to raise the number of Fellows from the traditional seven to the following eleven (the next available prime number):

Peter Blum & Carl Richter (*Ocean Drilling Program*)
Pleistocene glacial-interglacial changes in rock magnetic properties across the South Atlantic sector polar front
Maria T. Cioppa (*University of Windsor*)
Examining the magnetic characteristics of hydrocarbon reservoir and source rocks, Western Canada Sedimentary Basin

Monika Cogoini (*University of Oklahoma*)
Magnetic mineral formation in hydrocarbon exposed environments
Ulrike Draeger (*University of California-Santa Cruz*)
Characterizing the magnetic mineralogy and grain-size distribution of iron oxides in basaltic samples before and after CRM experiments
Ann Hirt (*ETH-Zürich*)
Magnetic properties of lepidocrocite and recent lake sediments
Ken Kodama (*Lehigh University*)
Testing for the presence of magnetosomes in Lake Ely sediments
Neil Linford (*Ancient Monuments Laboratory, English Heritage/University College London*)
Evidence of domestic fires in antiquity: A mineral magnetic approach based on recent experimental samples
Rick Oches (*University of South Florida*)
Quaternary sediment, environmental magnetism and paleoclimate: Filling in the gaps in loess records from Alaska and Mississippi

datafile access is more direct, and graphical output is enhanced.

This spring another significant advance is anticipated, with acquisition of a low-temperature subsystem for our Princeton "MicroMag" AGFM/VSM. This will enable rapid, sensitive measurement of hysteresis properties below room temperature. Hysteresis measurements, though technically possible on the Quantum instruments, are impractical due to the time required to vary magnetic fields in their superconducting magnets. Stay tuned for more details.

Low-temperature magnetometry has become an essential tool for rock-magnetic studies, and recent and pending equipment upgrades and acquisitions at IRM afford great new capabilities for such investigations, both in new sorts of measurement and in higher "throughput." If your research involves magnetism and/or earth materials, consider a visit to the nation's icebox for low-temperature measurements. (Special thanks to Ken Kodama for good-naturedly going along with our inane cover photo idea.)

*Actually, the new MPMS-XL is equipped with an airlock contraption, which we are still testing, but which potentially will allow sample changes at low temperature.

Özden Özdemir & David Dunlop (*University of Toronto at Mississauga*)
Low- and high-temperature properties of magnetite: Single crystals and sized PSD to MD grains
Hilde F. Passier (*Utrecht University*)
Integration of magnetic and geochemical data to study diagenetic iron mineral formation
Joseph E. Sabol (*University of Wisconsin-Eau Claire*)
Magnetic properties of manganese-substituted magnetite single crystals

The Institute for Rock Magnetism is dedicated to providing state-of-the-art facilities and technical expertise free of charge to any interested researcher who applies and is accepted as a Visiting Fellow. Short proposals are accepted semi-annually in spring and fall for work to be done in a 10-day period during the following half year. Shorter, less formal visits are arranged on an individual basis through the Facilities Manager.

The IRM staff consists of **Subir Banerjee**, Professor/Director; **Bruce Moskowitz**, Associate Professor/Associate Director; **Jim Marvin**, Senior Scientist; **Mike Jackson**, Senior Scientist and Facility Manager, and **Peat Solheid**, Scientist.

Funding for the IRM is provided by the **W. M. Keck Foundation**, the **National Science Foundation**, and the UofM.

The IRM Quarterly is published four times a year by the staff of the IRM. If you or someone you know would like to be on our mailing list, if you have something you would like to contribute (e.g., titles plus abstracts of papers in press), or if you have any suggestions to improve the newsletter, please notify the editor:

Mike Jackson
Institute for Rock Magnetism
University of Minnesota
291 Shepherd Laboratories
100 Union Street S. E.
Minneapolis, MN 55455D0128
phone: (612) 624-5274
fax: (612) 625-7502
e-mail: irm@geolab.geo.umn.edu
www.geo.umn.edu/orgs/irm/irm.html

I R M
Institute for Rock Magnetism

The UofM is committed to the policy that all people shall have equal access to its programs, facilities, and employment without regard to race, religion, color, sex, national origin, handicap, age, veteran status, or sexual orientation.

...Low-T

continued from page 7

transition temperature, cooling curves exhibited a much more complex and interesting behavior, controlled by both the K1 isotropic point and by the Verwey transition (see Özden's Visiting Fellow report on p 5 for more details).

Last but not least, the new XL has dramatically-improved control software. Programming experimental control sequences is now remarkably efficient,

Collector's Series #12

from *Hermann von Helmholtz*, by Helmut Rechenberg,
1994, VCH Verlagsgesellschaft

